Unravelling the pivotal role of atropisomerism for cellular internalization

Claire Donohoe[†‡], Fábio A. Schaberle[†], Fábio M. S. Rodrigues[†], Nuno P. F. Gonçalves[§], Christopher J. Kingsbury[‖], Mariette M. Pereira[†], Mathias O. Senge[‡,▽], Lígia C. Gomes-da-Silva[†*], Luis G. Arnaut[†*]

[†] – CQC, Coimbra Chemistry Center, University of Coimbra, Rua Larga, 3004-535 Coimbra, Portugal

[‡] – Medicinal Chemistry, Trinity Translational Medicine Institute, Trinity Centre for Health Sciences, St. James's Hospital, Trinity College Dublin, The University of Dublin, Dublin 8, Ireland

[§] – Luzitin SA, Ed. Bluepharma, S. Martinho do Bispo, 3045-016 Coimbra, Portugal

[‖] –School of Chemistry, Chair of Organic Chemistry, Trinity Biomedical Sciences Institute, 152-160 Pearse Street, Trinity College Dublin, The University of Dublin, Dublin 2, Ireland

[▽]– Institute for Advanced Study (TUM-IAS), Technical University of Munich, Lichtenbergstrasse 2a, 85748 Garching, Germany

Supporting information

Experimental Section

EXPERIMENTAL SECTION

1. Separation of redaporfin atropisomers by flash chromatography and analyses by reverse-phase high performance liquid chromatography (RP-HPLC)

Redaporfin, 5,10,15,20-tetrakis(2,6-difluoro-3-*N*-methylsulfamoylphenyl)bacteriochlorin atropisomeric mixture and the related 5,10,15,20-tetrakis(2,6-difluoro-3-*N*-methylsulfamoylphenyl)porphyrin (P11) were provided by Luzitin SA (Portugal). Redaporfin was dissolved in DMF and H_2O (4:1) (20 µg/µL) and sonicated for complete solubilization. Redaporfin atropisomers were separated by reversed-phase flash chromatography (Interchim Puriflash 420 system) using a reverse phase C18 column (Interchim PuriFlash Column, 15µ, C18 HP, 12 g). A solvent gradient of 60 to 95% acetonitrile (MeCN; Sigma) with Milli-Q H_2O was pumped at a constant flow rate of 1.5 mL/min over 70-90 minutes. The temperature of the column was kept at 23 °C and the detection of redaporfin was carried out at 743 nm. MeCN was removed from fractions under reduced pressure (water bath temperature max. = 40 °C) and removal of H_2O proceeded by lyophilization.
Samples from the obtained fractions were dissolved in a solution of MeCN and ammonium acetate buffer (6:4) (100 mM, pH 8-9.0) (Merck ACS reagent grade) and further submitted to reversed-phase HPLC analysis (Varian 920-LC Integrated Analytical HPLC) using a Phenomenex® brand RP-C18 column (4.6 × 25mm) at 23 ºC. A gradient of 60 to 95% MeCN with ammonium acetate buffer was used over 15 min at a constant flow rate of 1 mL/min. The four redaporfin bacteriochlorin and porphyrin (P11) atropisomers were detected at 743 nm and 414 nm, respectively.

2. ^{1}H NMR of separated atropisomers

^{1}H-NMR spectra were acquired on a Bruker Avance 400 spectrometer (400 MHz) using $CDCl_3$ or $(CD_3)_2SO$ as solvent. Chemical shifts are reported in ppm and referenced to residual solvent peak ($CHCl_3$; δH = 7.26 ppm or $(CH_3)_2SO$; δH = 2.50 ppm). The multiplicity is indicated as follows: s = singlet, d = doublet, t = triplet, q = quartet, m = multiplet and br = broad signal.

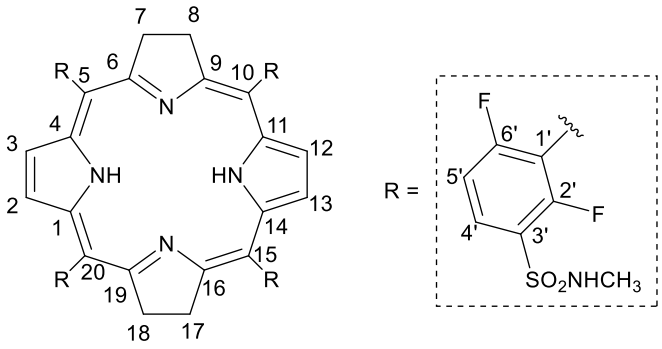

Sample (αβαβ)

^{1}H-NMR ($CDCl_3$, 400 MHz,) δ, ppm: 8.25-8.19 (m, 4H, $H_{4'}$); 8.00 (m, 4H, $H_{2,3,12,13}$); 7.30 (t, *J* = 8.2 Hz, 4H, $H_{5'}$); 4.69 (q, *J* = 5.1 Hz, 4H, N<u>H</u>CH_3); 4.03 (br, 8H, $H_{7,8,17,18}$); 2.79 (d, *J* = 5.2 Hz, 12H, NHC<u>H</u>$_3$); -1.37 (s, 2H, $NH_{pyrrole}$)

Sample ($\alpha_2\beta_2$)

^{1}H-NMR ($(CD_3)_2SO$, 400 MHz,) δ, ppm: 8.27-8.23 (m, 4H, $H_{4'}$); 8.23 (br, N<u>H</u>CH_3) 7.85-7.81 (m, 4H, $H_{2,3,12,13}$); 7.77 (t, *J* = 8.5 Hz, 4H, $H_{5'}$); 4.05 (br, 8H, $H_{7,8,17,18}$); 2.63 (d, *J* = 4.4 Hz, 12H, NHC<u>H</u>$_3$); -1.41 (s, 2H, $NH_{pyrrole}$)

Sample ($\alpha_3\beta$)

^{1}H-NMR ($CDCl_3$, 400 MHz,) δ, ppm: 8.27-8.22 (m, 4H, $H_{4'}$); 8.02-7.99 (m, 4H, $H_{2,3,12,13}$); 7.40-7.33 (m, 4H, $H_{5'}$); 4.75-4.69 (m, 4H, N<u>H</u>CH_3); 4.05 (br, 8H, $H_{7,8,17,18}$); 2.82-1.73 (m, 12H, NHC<u>H</u>$_3$); -1.39 (s, 2H, $NH_{pyrrole}$)

Sample (α_4)

^{1}H-NMR ($CDCl_3$, 400 MHz,) δ, ppm: 8.25-8.19 (m, 4H, $H_{4'}$); 7.93 (s, 4H, $H_{2,3,12,13}$); 7.30 (t, *J* = 8.1 Hz, 4H, $H_{5'}$); 4.82 (br, 4H, N<u>H</u>CH_3); 4.03 (br, 8H, $H_{7,8,17,18}$); 2.66 (br, 12H, NHC<u>H</u>$_3$); -1.50 (s, 2H, $NH_{pyrrole}$)

The assignments above agree with the literature.[1]

3. Crystal structure analyses

Crystals of the separated atropisomers of the porphyrin **P11** were grown by the following procedures: the α_4 sample was dissolved in acetonitrile and left to evaporate in a covered tube over the course of three months, whereupon crystals appeared at the base of the crystallization tube. The $\alpha_2\beta_2$ sample was dissolved in DMSO layered below ethyl acetate; however, no crystallization was observed on combination of the layers. Upon standing uncovered for a further month, crystals were evident on the wall of the tube, presumably induced by the slow diffusion of atmospheric water into the hygroscopic DMSO.

A diffraction pattern was collected on each of the two crystals using CuK_α radiation on a Bruker APEX-II DUO device, with extended collection times for the α_4 atropisomer to account for the poor diffraction evident at high angles across multiple crystal samples. Samples were held at 100.0(1) K with an Oxford CryoStream device. Data reductions were performed with the Bruker APEX3 package[2] and XPREP;[3] structures were solved with SHELXT[4] and refined with ShelXL[5] in the Shelxle GUI.[6] Images were generated with CrystalMaker X.[7] NSD analysis was performed with the online tool at https://www.sengegroup.eu/nsd.[8] Critical values related to the crystal structure refinement are in Table S1.

α_4

Reflections 4 0 0 and -13 1 6 were omitted based on disagreement with the model. Solvent was compensated for with SQUEEZE in PLATON;[9] quantity was assigned at 8 molecules per unit cell (4 per formula unit) based on compromise between available solvent area (indicating 10.2 /u.c.) and the residual electron density (indicating 7.5 /u.c.). Atoms were held to SIMU commands to generate realistic thermal parameters due to the limited available data. Hydrogen bonding arrangements were identified based on distance; relevant H-atoms were constrained with DFIX commands.

$\alpha_2\beta_2$

Two reflections were omitted on scaling. Non-rotamer disorder of the SO_2NHCH_3 group on C10 (S107-C111) was modelled as a two-site model, with EADP for C111/121, O108/118, O109/119 and SIMU for other atoms. SADI commands were used for these fragments to constrict to equal bond distances. C-bound H-atoms were fixed, N-H atoms constrained except H120, which was fixed. A large residual Q-peak could be observed next to the DMSO molecule - a two site disorder model was tried but failed to reach convergence, and the one-site model gave no additional issues.

Deposition Numbers 2124976 (for **P11-α_4**), 2124975 (for **P11-$\alpha_2\beta_2$**), contain the supplementary crystallographic data for this paper. This data is provided free of charge by the joint Cambridge

Crystallographic Data Centre and Fachinformationszentrum Karlsruhe http://www.ccdc.cam.ac.uk/structures Structures service.

4. Selective precipitation of redaporfin more "polar" atropisomers

P11 atropisomer mixture (5 mg) was dissolved in dichloromethane (CH_2Cl_2). The solution was combined with hexane and stirred for 1 minute. The precipitate observed was separated by centrifugation (4000 rpm, 15 minutes) to give sample X. The supernatant solvent was removed under reduced pressure to give sample Y. Both samples were analyzed by RP-HPLC in order to quantify the atropisomer relative amount in each sample. Each sample was dissolved in a solution of MeCN and ammonium acetate buffer (6:4) (100 mM, pH 9.0) (Merck ACS reagent grade) and further submitted to RP-HPLC (Elite Lachrom HPLC-DAD system with L-2455 Diode Array Detector) using a Purospher® STAR RP -C18 column (4.6 × 25mm, 0.1 μM) at 23 °C. A gradient of 60 to 95% MeCN with ammonium acetate buffer was used over 15 min at a constant flow rate of 1 mL/min. The four porphyrin atropisomers were detected at 414 nm. Figure S5 presents the RP-HPLC chromatograms with detection at 414 nm, revealing that the peaks of atropisomers αβαβ and $\alpha_2\beta_2$ increase in sample X with respect to the original sample of redaporfin, and that the peak of the atropisomer α_4 increases in sample Y with respect to the original sample. Table S4 presents the relative amounts of the fours atropisomers present in the initial redaporfin P11 sample and in fractions X and Y.

5. Barriers for C–C single bond rotation between macrocycle and aryl substituents

The stability of redaporfin atropisomers was investigated heating a sample of $\alpha_3\beta$ in dimethylformamide at high temperatures and for various periods of time as illustrated in Table S5. The interconversion of the atropisomers occurs rapidly at high temperatures without appreciable decomposition of the fluorinated sulfonamide bacteriochlorin. The relaxation time for each temperature was calculated[10] as the time of exponential decay according to

$$[A] - [A]_{eq} = ([A]_0 - [A]_{eq}) / e$$

where $[A]_0$ in the initial fraction of $\alpha_3\beta$ (99%), $[A]_{eq}$ is the fraction the statistical mixture in equilibrium (51%) and $e = 2.718$.

6. Photophysical and photochemical characterization of redaporfin atropisomers

Absorption spectra of redaporfin and P11 atropisomers were recorded on an Agilent Cary5000 UV-VIS-NIR spectrometer. Molar absorption coefficients (ε) were obtained from absorption measurements of three solutions of different concentrations, diluted from three stock 1 mM solutions with independently measured masses. The slope of the plot absorption *vs* concentration was used to calculate ε.

Further photophysical characterization of redaporfin atropisomers was carried out with absorption spectra recorded on a Shimadzu UV-2100 spectrophotometer. The fluorescence quantum yields were recorded in a Horiba-Jovin-Yvon Spex Fluorog 3-2.2 spectrophotometer using the near-infrared Hamamatsu R5509–42 photomultiplier, cooled to 193 K in a liquid nitrogen dewar. The fluorescence standard was 1,1′,3,3,3′,3′-hexamethylindotricarbocyanine iodide standard.[11] The wavelength of excitation, integration time and slits in one experiment were 743 nm, 0.8 s and 7 nm bandwidth (exc.) and 10 nm (em.), respectively. Samples and reference were prepared in ethanol with absorbance < 0.15 in the excitation wavelength. Triplet-triplet absorption spectra and the triplet lifetimes (τ_T) of redaporfin atropisomers were acquired with solutions with absorbances between 0.25 and 0.30, excited at 355 nm in an Applied Photophysics LKS 60 nanosecond flash photolysis kinetic spectrometer, using the third harmonic of a Spectra-Physics Quanta Ray GCR 130-01

Nd/YAG laser and a Hamamatsu 1P28 photomultiplier. The signals were recorded with a Hewlett-Packard Infinium oscilloscope (1 GS/s). Photodecomposition quantum yield (Φ_{PD}) was evaluated through photobleaching experiments involving irradiation of the bacteriochlorins in methanol:PBS (3:2) by a CW laser emitting at 745 nm (Omicron Laserage). The total output power of laser light was 640 mW. The time intervals between absorbance measurements ranged from minutes to hours of irradiation. Initial absorbances were ca. 1.0. The calculation followed the method previously described in the literature.[12]

Singlet oxygen quantum yields (Φ_{Δ}**)** were recorded using a method previously described in literature.[13] Phenalenone was used as a reference (Φ_{Δ} = 0.95 in methanol).[14] Singlet oxygen phosphorescence was measured at 1270 nm with a Hamamastu R5509-42 photomultiplier, cooled to 193 K in a liquid nitrogen dewar (Products for Research model PC176TSCE005), following pulsed laser excitation of aerated solutions at 355 nm, using an adapted Applied Photophysics spectrometer. A Newport cutoff filter below 1000 nm was employed to avoid fluorescence light. The quantum yields were calculated using the slope obtained from the phosphorescence signal dependence with laser energy

Aggregation studies were conducted with P11 atropisomers (2.5 μM) in pure DMSO or in water:DMSO (99.96:0.04). Absorption spectra in both solvents were recorded on an Agilent Cary 5000 UV-VIS-NIR spectrometer. Emission and excitation spectra were recorded on a Horiba-JY Fluoromax4 spectrofluorometer. P11 absolute values of fluorescence quantum yield were obtained for each atropisomer and were measured using the absolute method with a Hamamatsu Quantaurus QY absolute photoluminescence quantum yield spectrometer model C11347 (integration sphere).

7. Octanol/water partition coefficients (LogP$_{OW}$)

Redaporfin atropisomer LogP$_{OW}$ values were obtained using a modified shake-flask method. *N*-octanol was saturated with Milli-Q H_2O by preparing a mixture 1:1. The saturated *n*-octanol was separated after 24 h. A small sample of each compound was added to saturated *n*-octanol (4 mL) and vigorously mixed with an equal volume of Milli-Q H_2O (4 mL). Following centrifugation (3700 rpm, 3 minutes), phase partitioning was carried out. The H_2O phase was lyophilized (24 h) and re-suspended in 3 mL *n*-octanol. Emission spectra of both *n*-octanol solutions were recorded on a Horiba-JY Fluoromax4 spectrofluorometer with excitation at 505 nm. Area under curve (AUC, 720 -800 nm) was calculated and the log(*n*-octanol AUC / *n*-octanol used to re-suspend H_2O phase AUC) was used to calculate LogP$_{OW}$ values.

8. Cell culture and preparation of stocks solutions of the atropisomers

The CT26 (mouse colon carcinoma), U-2 OS (human osteosarcoma) and 4T1 (mouse breast cancer) cell lines were obtained from American Type Culture Collection Cells. Cells were maintained in Dulbecco's modified Eagle's medium (Sigma) supplemented with 10% heat inactivated fetal bovine serum (Gibco, Life Technologies) and 1% penicillin streptomycin (Sigma) in a humidified incubator with 5% CO_2 at 37 °C. Cells were detached using trypsin-EDTA solution (Sigma), counted, and seeded at the desired density in plates of the appropriate size for the different experiments.

A stock solution of each atropisomer (0.5 - 1 mM) was prepared with DMSO Hybri-Max^{TM} (Sigma) and stored at - 20 °C. Before each experiment, the stock solutions of atropisomers were diluted in culture medium at the desired concentration and added to the cells. Due to limited amounts of redaporfin atropisomers, in some experiments, P11 atropisomers were used instead as their relative biological activities can be considered as analogous to the bacteriochlorin atropisomers.

9. Cell viability using the resazurin reduction assay

CT26 (5000 cells/ well), U-2 OS (7000 cells/ well) 4T1 (7000 cells/ well) and HaCat (10000 cells/ well) cells were seeded in 96-well plates. 24 h later, cells were treated with the single atropisomers in a concentration range from 2.5 to 0.08 μM for 24 h. After a washing step with medium, cells were illuminated with a light-emitting diode (LED) at 740 nm or 410 nm, respectively for redaporfin or P11 atropisomers. The overlap between the LED and the photosensitizers spectra was calculated in order to obtain accurate light doses.[15] A light dose of 0.2 J/cm^2 was delivered for redaporfin atropisomers whereas 0.05 J/cm^2 or 0.0125 J/cm^2 were applied in those experiments involving P11 atropisomers. Cellular viability was evaluated 24 h post-illumination using the resazurin reduction assay.[16] For this, cells were incubated with resazurin with DMEM (0.01 mg/mL, Sigma-Aldrich) for approximately 2 h and the fluorescence of the metabolic product, resorufin, was recorded with a microplate reader (Biotek Synergy HT) using 528/20 nm excitation and 590/35 nm emission filters. The level of resazurin metabolization by the untreated cells (Ctrl) was assumed as 100% viability. Parallel experiments were conducted with higher concentrations of the atropisomers (1.25 to 20 μM) to assess the safety of the different atropisomers in the absence of light (dark toxicity).

10. Cellular internalization

CT26 (20,000 cells/ well), U-2 OS (30,000 cells/ well), 4T1 (40,000 cells/ well) and HaCat (100000 cells/ well) cells were seeded in 24-well plates. After 24 h, cells were incubated with the single atropisomers at a concentration of 2.5 μM. At different time points (2, 4, 8, 16 and 24 h), cells were washed with culture medium, detached with trypsin-EDTA and fixed in paraformaldehyde (PFA) 3.7% (w/v) for 20 - 30 minutes. After an additional washing step with PBS, cells were resuspended in PBS and analyzed by flow cytometry using a Novocyte® TM 3000 (ACEA). Redaporfin fluorescence was measured upon excitation with the 488 nm laser and detection was performed using the 780/60 nm filter. For P11, the 405 nm laser was used with detection on the channel of 615/24 nm. An average of 10,000 events were collected and data is presented as mean fluorescence normalized to the mean fluorescence of untreated cells.

In parallel experiments, cells were incubated with the single atropisomers (2.5 μM) for 24 h, washed and submitted to cell lysis using DMSO with Triton X 1% (v/v). To quantify the absolute amount of internalized atropisomers, a calibration curve of the single atropisomers was also prepared in the lysis buffer. After centrifugation to separate cellular debris, the obtained supernatant (containing the internalized atropisomers) was analyzed for detection of fluorescence. This was carried out with a microplate reader (Biotek Synergy HT) using 508/20 nm excitation and 760/34 nm emission filters for redaporfin and 420/50 nm excitation and 645/40 nm emission filters for P11. The amount of each atropisomer was extrapolated from the calibration curve and normalized to the total amount of protein. Protein quantification was carried out using the Pierce™ BCA Protein Assay Kit according to the manufacturer's instructions (Thermo Scientific).

Subcellular distribution of P11 atropisomers was evaluated in U-2 OS cells stably expressing CALR-GFP or GALT1-GFP, which were a kind gift from Prof. Guido Kroemer (Université Paris Descartes). Cells (17,000 cells/ well) were seeded in an μ-Slide 8-well treated plate (Ibidi) and left to adapt for 24 h. Then, cells were incubated with the single atropisomers (10 μM) for 24 h, followed by a washing step and fixation with PFA 3.7% (w/v). Images were acquired with a Carl Zeiss LSM 710 Confocal Microscope. GFP was detected using a 488 nm laser and 525/50 nm emission filter while P11 was detected using a 405 nm laser and 605/70 nm emission filter

11. Mechanism of cellular internalization

To evaluate the temperature dependence of atropisomer cellular uptake , 4T1 cells (50,000 cells/well) were seeded in 24-well plates 24 h later, 4T1 cells were incubated with the P11 atropisomers (2.5 μM) at 37 °C or at 4 °C, for 4 h. In parallel experiments, the ATP dependence of uptake was evaluated. For this, cells were washed with glucose deficient DMEM and incubated with 2-deoxy-D-glucose (20 mM) for 1 h at 37 °C. ATP-

depleted cells were washed with glucose deficient DMEM followed by incubation with the single P11 atropisomers (2.5 μM), for 2 h. Pierce™ Recombinant GFP Protein (40 nM) was included as a positive control of endocytosis. ATP depletion was confirmed using an ATP-Assay Kit (Abcam, ab8355) according to the manufacturer´s instructions. Finally, the impact of plasma proteins on the atropisomer uptake was also evaluated. Briefly, FBS deficient DMEM supplemented with bovine serum protein (4 and 8 mg/mL BSA, Sigma), human low-density lipoprotein (0.02 and 0.04 mg/mL LDL, Calbiochem) or human high-density lipoprotein (0.02 and 0.04 mg/mL HDL, Sigma) was used to prepare 2.5 μM solutions of atropisomers. These solutions were maintained at 37 °C for 30 min to favor potential interactions between the proteins and the atropisomers. Cells were then incubated with the protein-supplemented medium containing the atropisomers for 4 h at 37 °C. In these experiments, cellular internalization was evaluated by flow cytometry as described above.

12. Interaction of redaporfin atropisomers with 1-palmitoyl-2-oleoyl-*sn*-glycero-3-phosphocholine (POPC) liposomes

A stock solution of each atropisomer (0.5 mM) was prepared in DMSO which was further diluted in PBS to a final concentration of 5 μM (1% DMSO). To this solution, POPC liposomes were added at a final concentration of 0.125 mM. After 20 min of incubation, fluorescence was measured with a microplate reader (Biotek Synergy HT) using 528/20 nm excitation and 590/35 nm emission filters. This was followed by 6 additions of POPC liposomes until the stabilization of redaporfin fluorescence (final POPC concentration of 3.25 mM).

13. Atropisomer internalization by cells of the tumor microenvironment

All the animal experiments were approved by the Portuguese Animal and Food Authority (DGAV authorization 0421/000/000/2020). Tumors were established by subcutaneous (sc) injection of 350,000 CT26 cells in the right flank of female BALB/c mice ca. 10 - 12 weeks old (20 g).

When tumor diameter reached ca. 5 mm, P11 atropisomers (2.5 mg/ kg) were delivered intravenously (via the tail vein) as a formulation of saline : DMSO : Kolliphor®EL (97 : 1: 2% v/v). Relative micelle size was determined by acquisition of hydrodynamic radius (z-average) by dynamic-light scatter (Zetasizer Nano Series). Tumors were collected 24, 48 and 72 h after the atropisomers administration and incubated with 1 mL of Liberase (Sigma, 16 μg/ mL) and Deoxyribonuclease I from bovine pancreas (Sigma, 8300 U/mL) for 1 h at 37 °C. The obtained tumor cell suspension was resuspended in DMEM, passed through a 70 μm cell strainer and washed with PBS. Cells were then incubated with the Zombie-violet™ live dead stain (1:500) (Biolegend) for 15 minutes at 4 °C in the dark. After washing with cold PBS, cells were immediately analyzed by flow cytometry (Novocyte 3000, ACEA). The Zombie-violet™ signal was detected upon excitation with the 405 nm laser and detection at the channel 445/45 nm. P11 fluorescence was acquired using the 405 nm laser (excitation) with detection at the channel of 615/24 nm. An average of 5000 events negative to Zombie-violet™ (live cells) were collected and data is presented as mean fluorescence normalized to the signal of tumors suspensions from untreated mice.

14. Treatment of BALB/c mice bearing CT26 tumors with PDT using redaporfin atropisomers

Tumors were established by subcutaneous injection of 350,000 CT26 cells in the right flank of female BALB/c mice ca. 10 - 12 weeks old (20 g) or male BALB/c ca. 10 – 12 weeks (25 g). Treatments were performed when tumors reached ca. 5 mm. Redaporfin atropisomers were delivered intravenously (via the tail vein) as a formulation of saline : EtOH : Kolliphor®EL (98.5 :1 : 0.5% v/v). Relative micelle size was determined by acquisition of hydrodynamic radius (z-average) by dynamic-light scatter (Zetasizer Nano Series). The illumination was performed with a laser at 749 nm (Omicron Laserage). Vascular-PDT (0.45 mg/ kg, DLI = 15 min, 40 J/cm^2 @ 137 mW/cm^2, 1.33 cm^2 area of illumination) and cellular-PDT (0.35 mg/kg, DLI = 24 h, 60 J/cm^2 @ 137 mW/cm^2, 1.33 cm^2 area of illumination) protocols were optimized in order to obtain the best therapeutic outcomes without significant toxicity. Tumors were measured twice a week with a caliper and the volume was calculated using the formula $V = (a \times b^2)/2$, where *a* corresponds to the major diameter and *b* to the minor diameter. The humane endpoint of tumor size followed was major diameter > 12 mm. Cured mice were subjected to re-challenge with subcutaneous injection of 350,000 CT26 cells ca. 6 weeks after PDT treatment.

15. Skin photosensivity

Hair from the dorsum of male BALB/c mice ca. 10 - 12 weeks old was removed using depilatory cream followed by intravenous administration of redaporfin mixture (0.45 mg/kg) or the α_4 atropisomer (0.45 mg/kg). After three or seven days, skin areas of 0.5 cm^2 were illuminated for 15 min (90 J /cm^2) or 30 min (180 J /cm^2) using a solar simulator (Oriel with global filter AM 1.5, 100 mW/cm^2). Mice without administration of any compound were included as control. Skin effects, specifically erythema, were measured by means of a Mexameter (Courage-Khazaka).

16. Statistical analysis

Data from cellular studies are presented as the mean ± standard error mean (SEM) of 2-3 independent experiments, each one in triplicates. Unpaired student's t test, one- or two-way ANOVA were used when indicated to determine statistically significant differences between the atropisomer α_4 mean and the other atropisomers. Survival analysis of PDT-treated mice was performed by means of a Kaplan–Meier estimator with long-rank (Mantel-Cox) test to evaluate the significance of the differences between different PDT treated groups.[17]

A

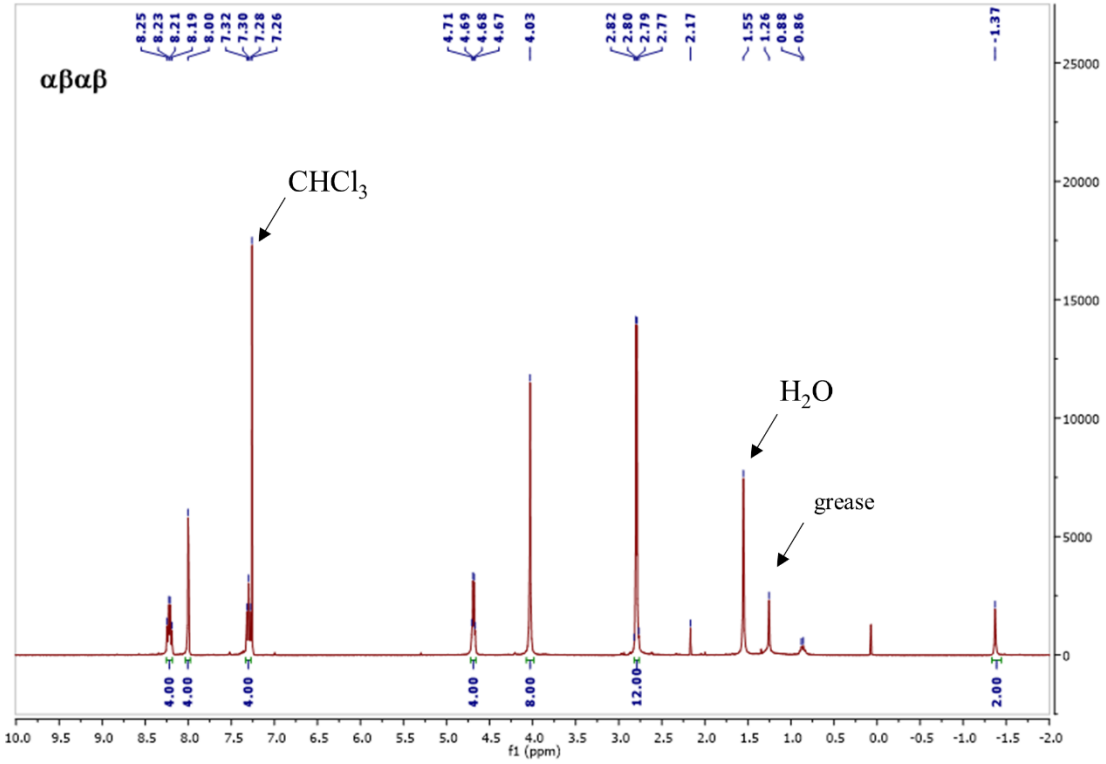

B

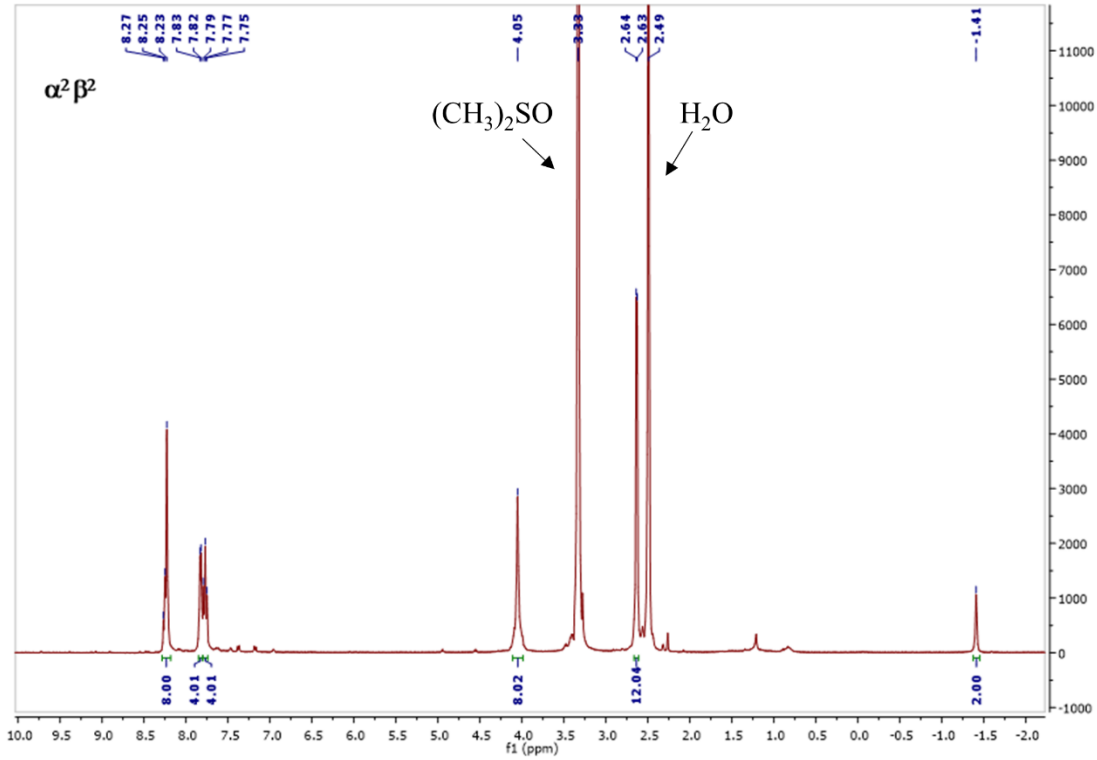

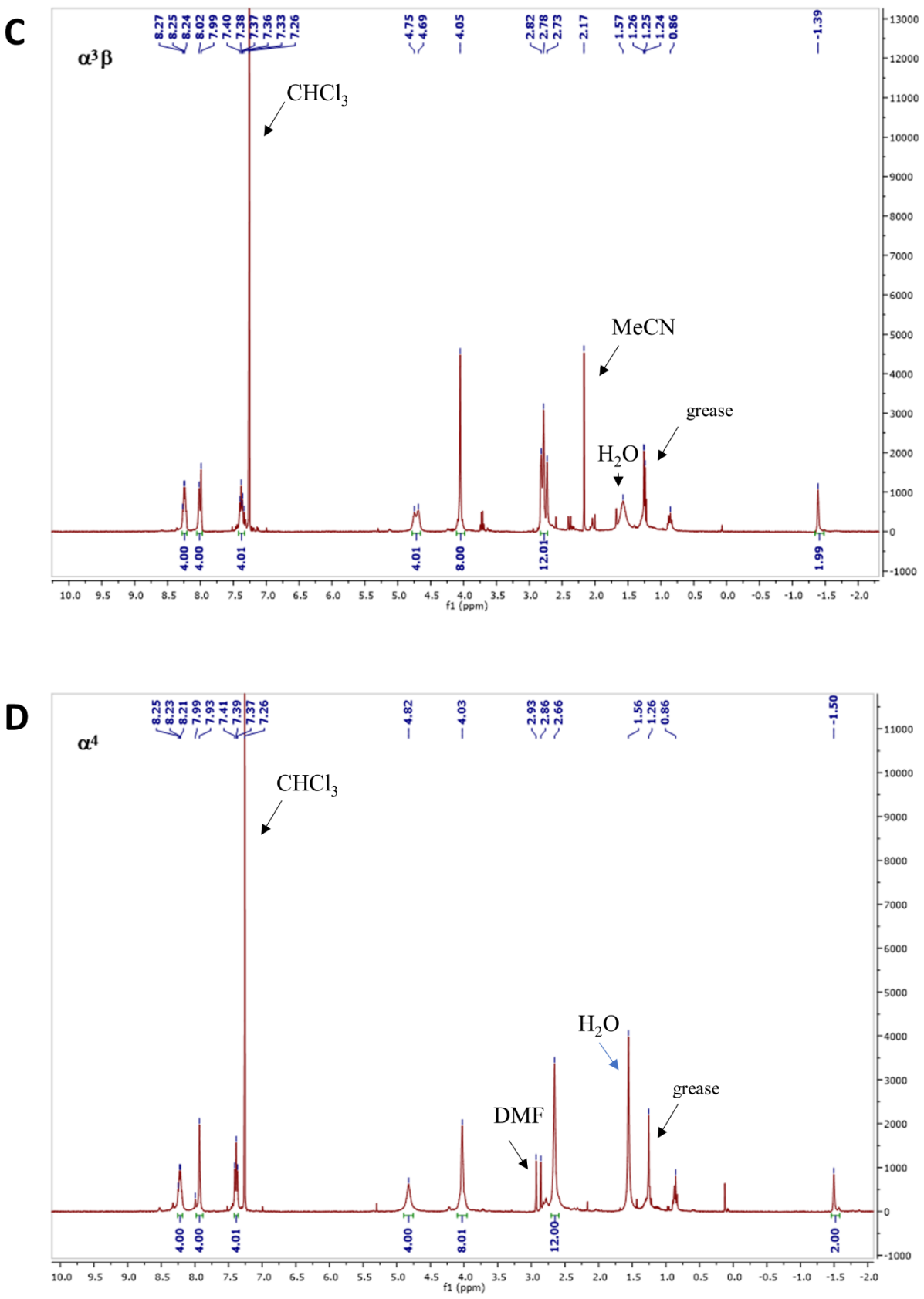

Figure S1. ^{1}H NMR spectra of redaporfin atropisomers. (A) Sample αβαβ, (B) sample $\alpha_2\beta_2$, (C) sample $\alpha_3\beta$ and (D) sample α_4.

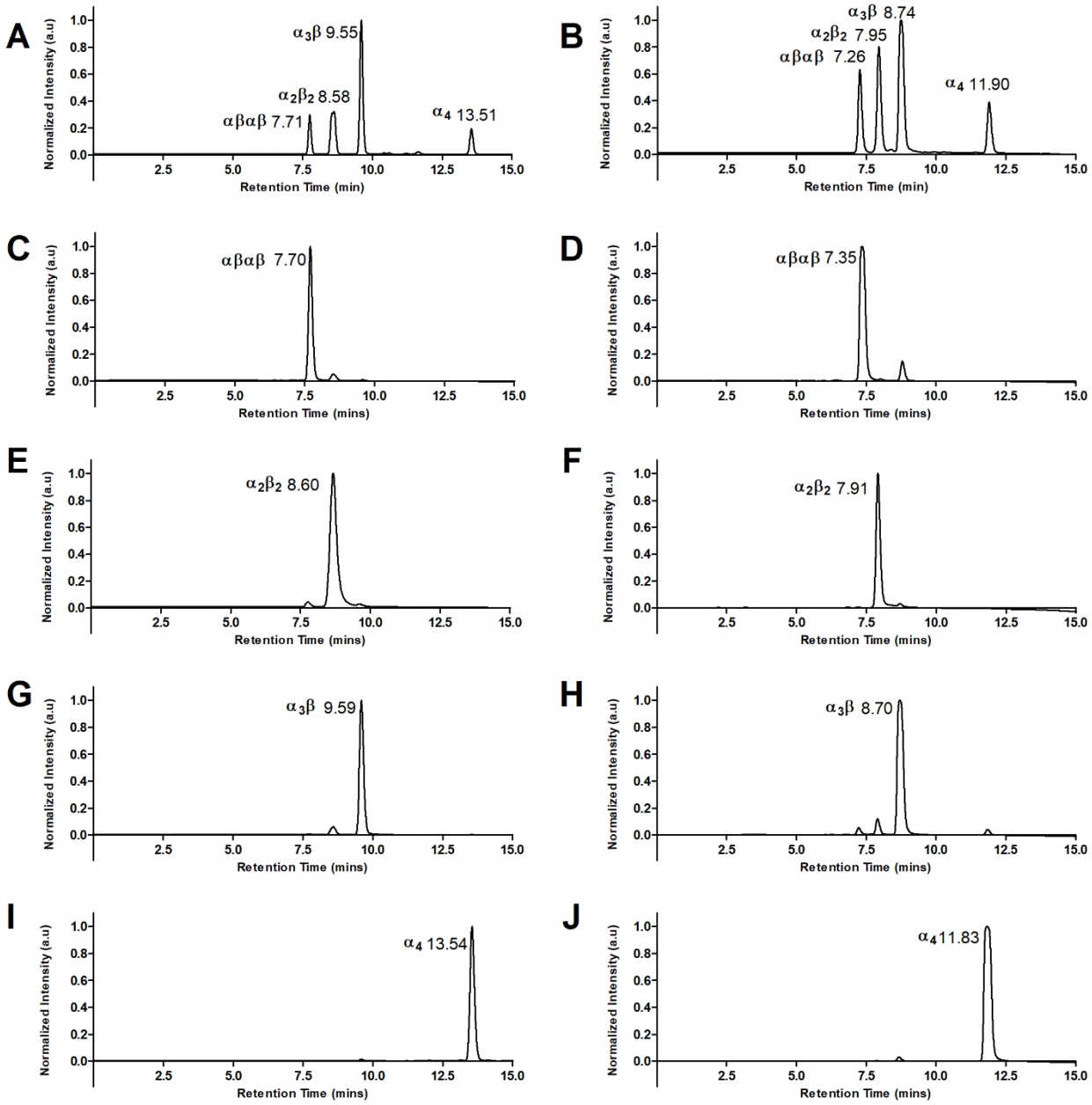

Figure S2. HPLC chromatograms of redaporfin and P11 porphyrin atropisomers. (A) Redaporfin mixture, (C) sample αβαβ, (E) sample $\alpha_2\beta_2$, (G) sample $\alpha_3\beta$ and (I) sample α_4. (B) P11 mixture, (D) sample P11 αβαβ, (F) sample P11 $\alpha_2\beta_2$, (H) sample P11 $\alpha_3\beta$ and (J) sample P11 α_4.

Table S1. Crystallographic data associated with P11 atropisomers.

Identification code	P11 $\alpha_2\beta_2$	P11 α_4
CCDC deposition number	2124975	2124976
Internal Code	CJK_013	CJK_059
Chemical formula	$C_{52}H_{46}F_8N_8O_{10}S_6$	$C_{52}H_{40}F_8N_{10}O_8S_4$
Formula weight	1287.33 g/mol	1213.18 g/mol
Temperature	100(2) K	100(2) K
Wavelength	1.54178 Å	1.54178 Å
Crystal size	0.039 × 0.047 × 0.074 mm	0.032 × 0.064 × 0.103 mm
Crystal system	monoclinic	monoclinic
Space group	P 1 21/c 1	C 1 2/c 1
Unit cell dimensions	a = 12.0820(7) Å	a = 32.616(3) Å
	b = 17.5200(9) Å	b = 12.4059(12) Å
	c = 12.8830(8) Å	c = 13.9874(13) Å
	α = 90°	α = 90°
	β = 100.933(4)°	β = 109.291(5)°
	γ = 90°	γ = 90°
Volume	2677.5(3) $Å^3$	5342.0(9) $Å^3$
Z	2	4
Density (calculated)	1.597 g/cm^3	1.508 g/cm^3
Absorption coefficient	3.207 mm^{-1}	2.451 mm^{-1}
F(000)	1324	2488
Theta range for data collection	3.73 to 68.39°	2.87 to 69.35°
Index ranges	-14<=h<=13, -21<=k<=21, -15<=l<=15	-38<=h<=39, -14<=k<=10, -16<=l<=16
Reflections collected	23203	10652
Independent reflections	4898 [R(int) = 0.0990]	4125 [R(int) = 0.0994]
Coverage of independent reflections	99.5%	82.6%
Absorption correction	Multi-Scan	Multi-Scan
Max. and min. transmission	0.7531 and 0.5629	0.7531 and 0.5721
Structure solution technique	direct methods	direct methods
Structure solution program	SHELXT 2018/2 (Sheldrick, 2018)	SHELXT 2018/2 (Sheldrick, 2018)
Refinement method	Full-matrix least-squares on F^2	Full-matrix least-squares on F^2
Refinement program	SHELXL-2018/3 (Sheldrick, 2018)	SHELXL-2018/3 (Sheldrick, 2018)
Function minimized	$\Sigma\ w(F_o^2 - F_c^2)^2$	$\Sigma\ w(F_o^2 - F_c^2)^2$
Data / restraints / parameters	4898 / 148 / 410	4125 / 706 / 349
Goodness-of-fit on F^2	1.065	1.071
Final R indices	R1 = 0.0683, wR2 = 0.1931 3092 data; I>2σ(I)	R1 = 0.1253, wR2 = 0.3011 1892 data; I>2σ(I)
	R1 = 0.1060, wR2 = 0.2157 all data	R1 = 0.2188, wR2 = 0.3540 all data
Weighting scheme	$w=1/[\sigma^2(F_o^2)+(0.1201P)^2+0.0553P]$ where $P=(F_o^2+2F_c^2)/3$	$w=1/[\sigma^2(F_o^2)+(0.1815P)^2]$ where $P=(F_o^2+2F_c^2)/3$
Largest diff. peak and hole	0.983 and -0.811 $eÅ^{-3}$	1.466 and -0.549 $eÅ^{-3}$
R.M.S. deviation from mean	0.097 $eÅ^{-3}$	0.132 $eÅ^{-3}$

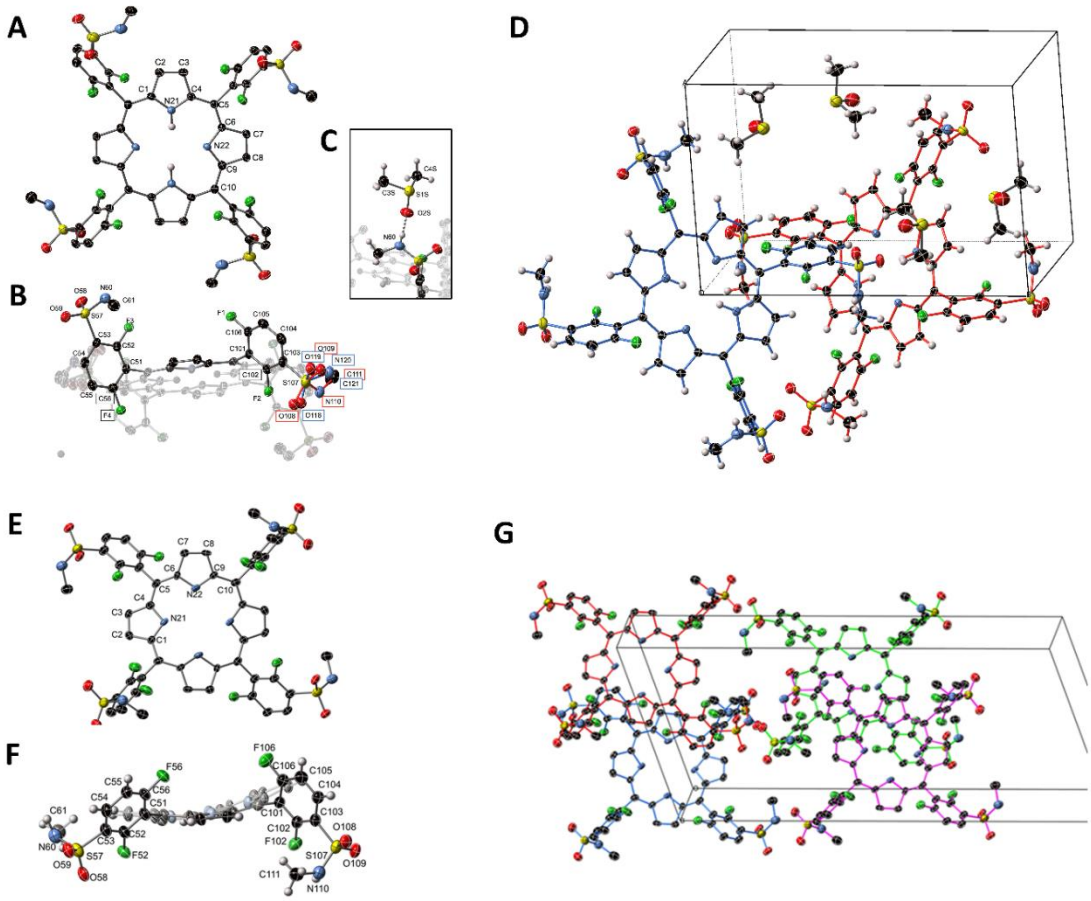

Figure S3. Crystal structures of P11 $\alpha_2\beta_2$·2Me$_2$SO and P11α_4·4MeCN.
(**A-C**) Labelled atom positions from the crystal structure of $\alpha_2\beta_2$·2Me$_2$SO: **(A)** porphyrin ring, **(B)** side-chains and, **(C)** DMSO solvate. Thermal ellipsoids are shown at the 50% occupancy level, H-atoms are represented as spheres or omitted. The disordered O108-C111 (red, 62.4(5) %) and O118-C121 (blue, 37.6(5) %) are shown in **(B)** and omitted elsewhere. **(D)** P11 molecules (Z = 2) within the unit cell of $\alpha_2\beta_2$-1·2Me$_2$SO. Two equivalent P11 porphyrin molecules are shown in red and blue bonds, with solvate molecules in black. The minor disorder fraction has been omitted and ellipsoids are shown at the 50% probability level**.**
(E-F) Labelled atom positions from the crystal structure of α_4·4MeCN: (**E**) the porphyrin ring and **(F)** the side-chains. Thermal ellipsoids are shown at the 50% occupancy level, H-atoms are represented as spheres or omitted. **(G)** P11 molecules (Z = 4) within the unit cell of α_4·4MeCN. The four equivalent P11 porphyrin molecules are shown in red, blue, green and magenta bonds, with solvate compensated by the SQUEEZE technique.

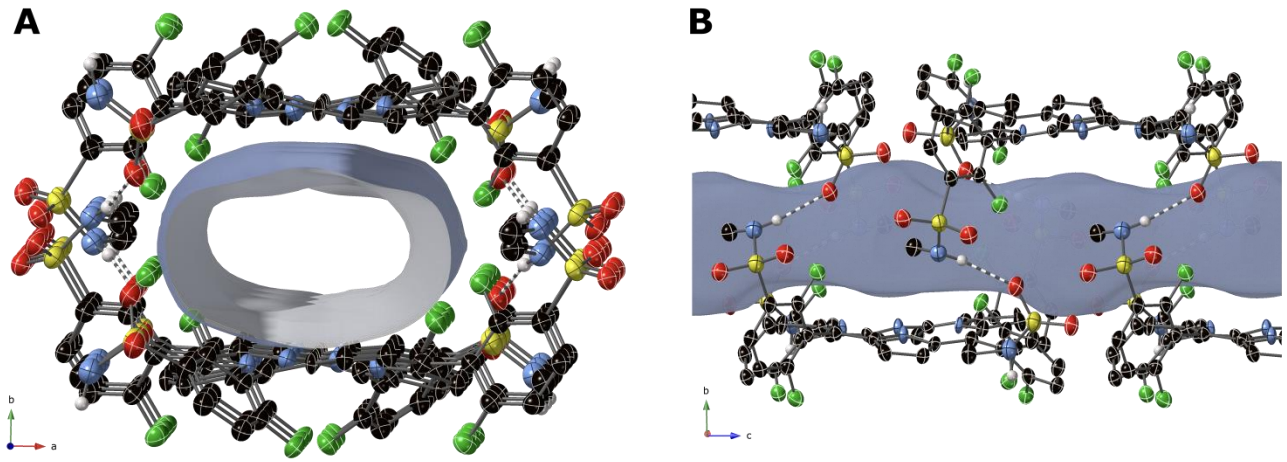

Figure S4. An indication of the solvent-filled channel (blue/grey) in the crystal structure of P11 α_4·4MeCN with a 1.4 Å probe radius, viewed perpendicular to the (A) *ab*- plane and (B) *bc*- plane. Hydrogen bonding interactions are indicated with striped bonds.

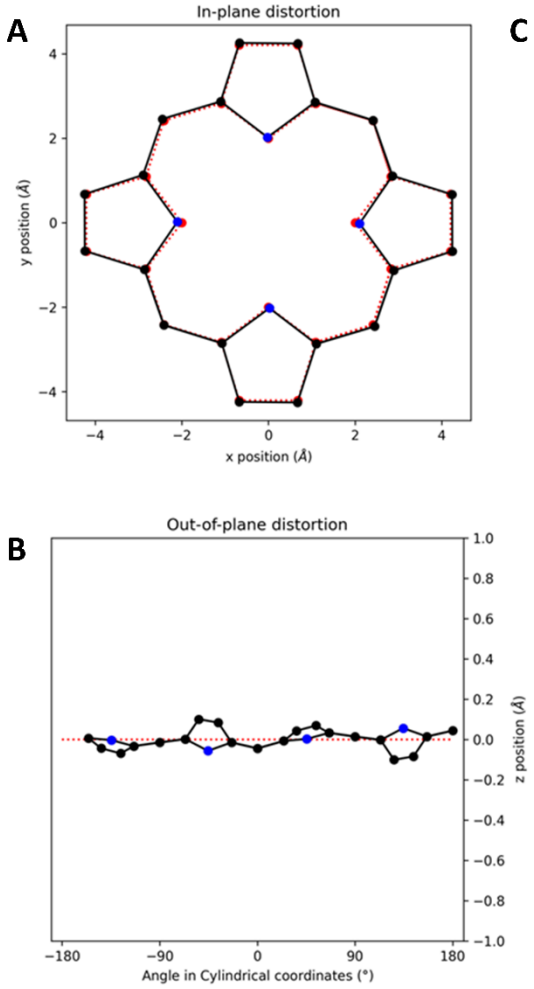

C **Table S2. NSD result generated from file cjk_013_mp_a.pdb at Wed Apr 14 21:39:08 2021**
Summary of the NSD (in Å):

basis	Δ_{ip}	δ_{ip}	B_{2g}	B_{1g}	$E_u(x)$	$E_u(y)$	A_{1g}	A_{2g}
min.	0.23	0.00	-0.08	0.03	0.00	0.00	0.22	0.00
ext.	0.24	0.00	-0.08	0.03	0.00	0.00	0.22	0.00
			-0.01	0.06	0.00	0.00	-0.02	-0.01
total	0.26	0.00	-0.08	0.04	0.00	0.00	0.22	0.00
			-0.01	0.06	0.00	0.00	-0.02	-0.01
			0.00	0.06	0.00	0.00	0.05	0.01
			0.00	0.01	0.00	0.00	-0.01	-0.01
			-0.01	0.01	0.00	0.00	0.01	0.00
			0.00	0.02	0.00	0.00	0.02	
					0.00	0.00		
					0.00	0.00		
					0.00	0.00		
					0.00	0.00		
					0.00	0.00		
comp.	0.26	0.00	0.08	0.10	0.00	0.00	0.23	0.02

basis	Λ_{oop}	δ_{oop}	B_{2u}	B_{1u}	A_{2u}	$E_g(x)$	$E_g(y)$	A_{1u}
min.	0.22	0.00	0.00	0.00	0.00	-0.09	-0.20	0.00
ext.	0.22	0.00	0.00	0.00	0.00	-0.09	-0.20	0.00
			0.00	0.00	0.00	0.02	-0.04	0.00
total	0.22	0.00	0.00	0.00	0.00	-0.09	-0.20	0.00
			0.00	0.00	0.00	0.02	-0.04	0.00
			0.00	0.00	0.00	0.02	0.02	
						0.01	0.00	
						-0.01	-0.01	
comp.	0.22	0.00	0.00	0.00	0.00	0.09	0.20	0.00

Figure S5. Results of an individual structure query to an NSD (Normal-coordinate structural decomposition) web interface for the P11 $\alpha_2\beta_2$ atropisomer. Symmetry of the porphyrin macrocycle demonstrated: **(A)** in-plane and **(B)** out-of-plane skeletal plots of the porphyrin core. Porphyrin is represented (black (C) and blue (N)) with the reference structure (CuTPP) in red dotted lines. **(C)** Table S2 representing NSD result for P11 $\alpha_2\beta_2$ atropisomer.

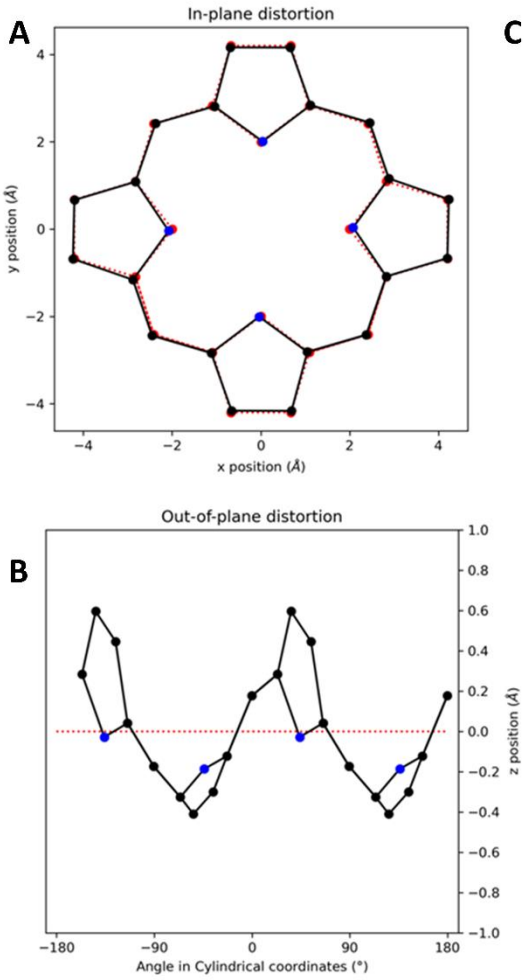

C **Table S3; NSD result generated from file cjk_059_sq.pdb at Mon Feb 1 13:46:09 2021**
Summary of the NSD (in Å):

basis	Δ_{ip}	δ_{ip}	B_{2g}	B_{1g}	$E_u(x)$	$E_u(y)$	A_{1g}	A_{2g}
min.	0.18	0.01	0.15	0.09	0.00	0.00	0.04	-0.01
ext.	0.21	0.00	0.15	0.09	0.00	0.00	0.04	-0.01
			0.03	0.08	0.00	0.00	-0.04	0.06
total	0.24	0.00	0.15	0.09	0.00	0.00	0.05	-0.01
			0.03	0.08	0.00	0.00	-0.04	0.06
			0.01	0.00	0.00	0.00	0.09	-0.01
			0.02	0.01	0.00	0.00	0.00	0.00
			0.00	0.02	0.00	0.00	0.00	0.02
			-0.03	0.03	0.00	0.00	0.01	
					0.00	0.00		
					0.00	0.00		
					0.00	0.00		
					0.00	0.00		
					0.00	0.00		
comp.	0.24	0.00	0.16	0.13	0.00	0.00	0.11	0.06

basis	Δ_{oop}	δ_{oop}	B_{2u}	B_{1u}	A_{2u}	$E_g(x)$	$E_g(y)$	A_{1u}
min.	1.49	0.00	1.36	0.51	-0.33	0.00	0.00	-0.04
ext.	1.49	0.00	1.36	0.51	-0.33	0.00	0.00	-0.04
			-0.03	0.00	-0.01	0.00	0.00	0.00
total	1.49	0.00	1.36	0.51	-0.33	0.00	0.00	-0.04
			-0.03	0.00	-0.01	0.00	0.00	0.00
			-0.03	-0.02	0.01	0.00	0.00	
						0.00	0.00	
						0.00	0.00	
comp.	1.49	0.00	1.36	0.51	0.33	0.00	0.00	0.04

Figure S6. Results of an individual structure query to an NSD (Normal-coordinate structural decomposition) web interface for the P11 α_4 atropisomer. Symmetry of the porphyrin macrocycle demonstrated: **(A)** in-plane and **(B)** out-of-plane skeletal plots of the porphyrin core. Porphyrin is represented (black (C) and blue (N)) with the reference structure (CuTPP) in red dotted lines **(C)** Table S3 representing NSD result for P11 α_4 atropisomer.

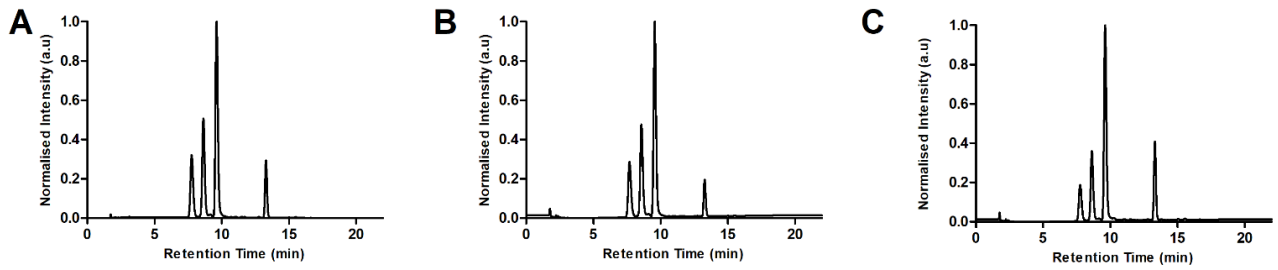

Figure S7. Selective precipitation of more polar atropisomers by addition of hexane to the statistical mixture of P11 atropisomers dissolved in dichloromethane. (A) RP-HPLC of the atropisomeric mixture initially present in dichloromethane. (B) RP-HPLC of the fraction X which precipitated upon addition of hexane. (C) RP-HPLC of the fraction Y which remained in the dichloromethane:hexane (1:1) solvent mixture.

Table S4. Relative atropisomer contents of P11 sample and of samples X (precipitate) and Y (soluble in less polar solvent mixture) calculated with chromatogram peak areas. Mean of value of two independent experiments.

	Relative Atropisomer Proportion (%)		
	P11	Sample X	Sample Y
αβαβ	16.1	17.2	11.5
$\alpha_2\beta_2$	24.8	27.6	20.5
$\alpha_3\beta$	48.4	47.9	51.4
α_4	10.7	7.4	16.8

Table S5. **Relative atropisomer contents after heating a $\alpha_3\beta$ sample in dimethylformamide.** The indicated periods of time and temperatures, open to the atmosphere, were tested.[1]

	Relative Atropisomer Proportion (%)				
	Initial	Temperature Time	Temperature Time	Temperature Time	Temperature Time
		85 °C 12 h	140 °C 5 min	140 °C 10 min	140 °C 20 min
Assay		(%w/w)	(%w/w)	(%w/w)	(%w/w)
αβαβ	-	5	14	9	12
$\alpha_2\beta_2$	1	14	19	20	23
$\alpha_3\beta$	99	74	60	58	52
α_4	-	7	5	11	11

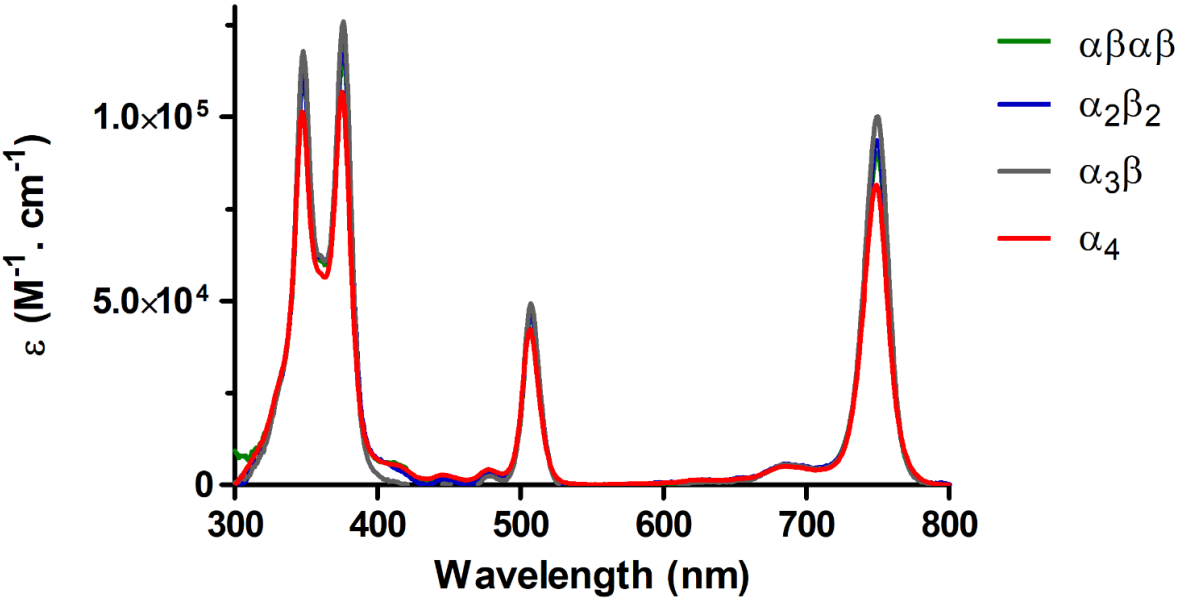

Figure S8. Absorbance spectra of redaporfin atropisomers in DMSO.

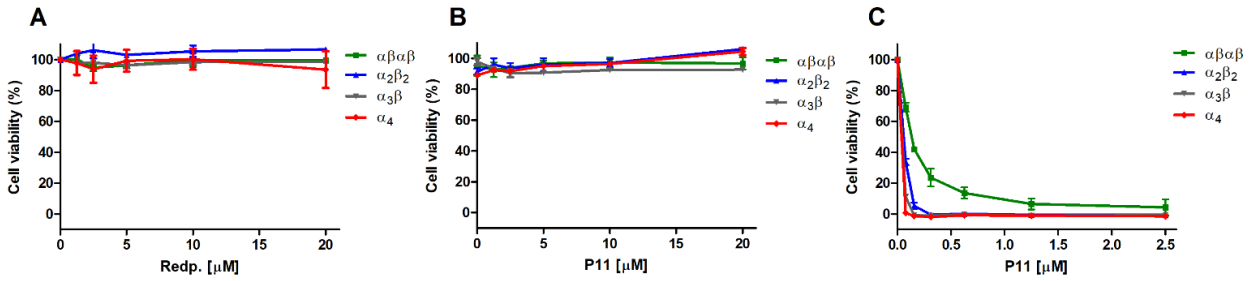

Figure S9. Lack of dark toxicity of redaporfin and P11 porphyrin atropisomers in 4T1 cells and phototoxicity in U-2 OS cells. (A) Redaporfin and **(B)** P11 atropisomers cellular viability in 4T1 cells following 24 h incubation. Result indicates the mean ± SEM of 2 independent experiments. **(C)** U-2 OS treated with P11 atropisomers and DL = 0.05 J/cm^2 Results indicate mean ± SD of a single representative experiment. Statistical significance was evaluated using two-way ANOVA *versus* the α_4 atropisomer, no symbol $p > 0.05$.

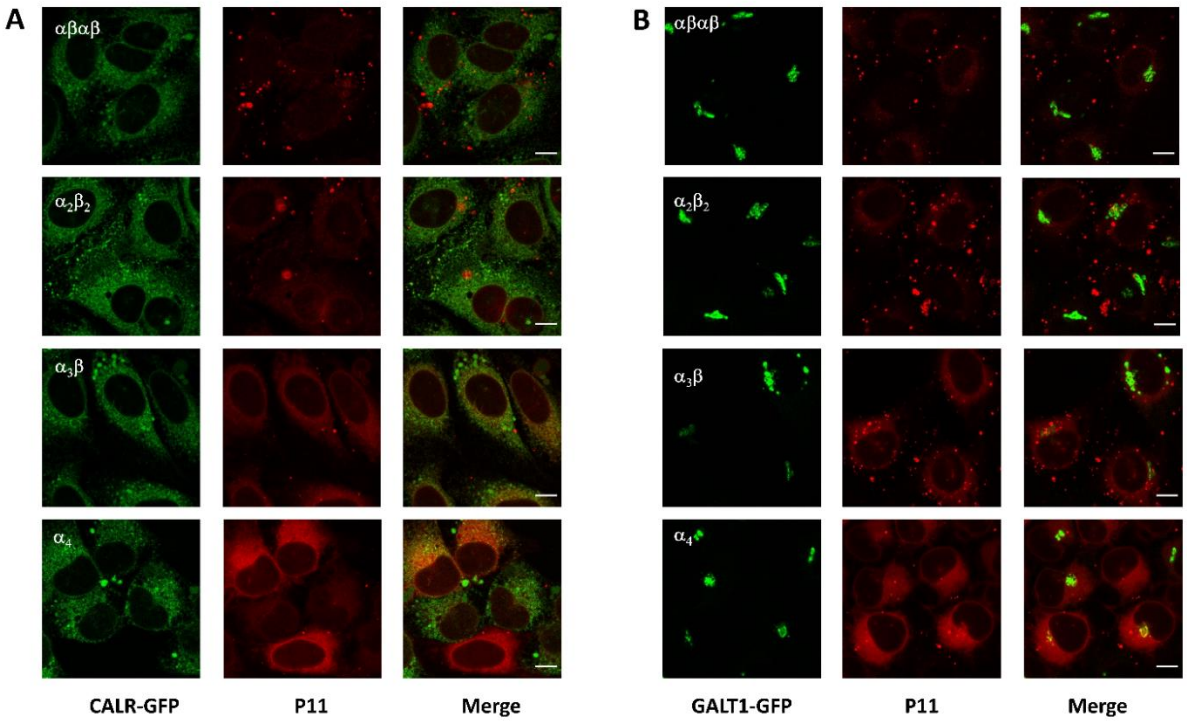

Figure S10. **P11 atropisomers preferentially accumulated at the endoplasmic reticulum and Golgi compartments.** Representative images of the co-localization of P11 atropisomers (red) with markers of **(A)** the endoplasmic reticulum (CALR-GFP) and **(B)** Golgi (GALT1-GFP) in U-2 OS cells. For each experiment, 10 µM of each atropisomers were used and images were acquired using the same settings. Brightness and contrast were adjusted using image-J varying degrees for each atropisomer to visualize subcellular targeting. Scale bar represents 10 µm.

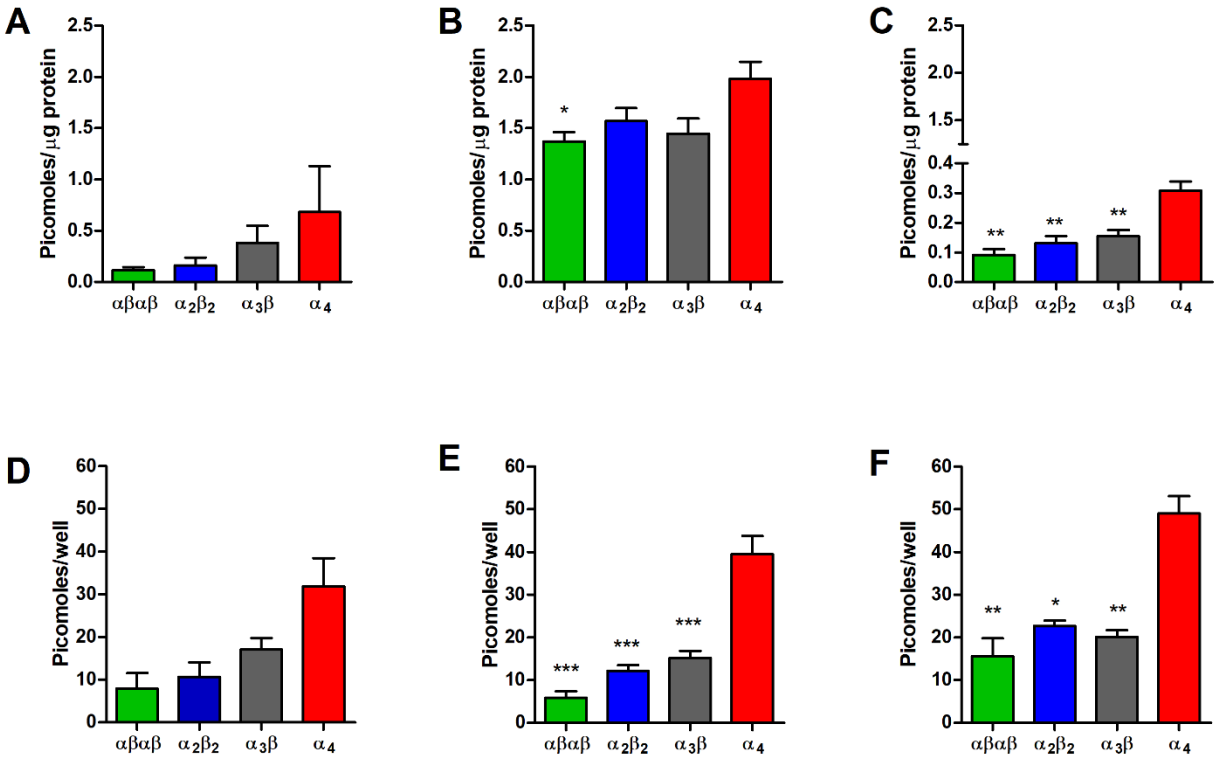

Figure S11. Quantification of redaporfin and P11 atropisomers in the supernatant of cancer cells. Cancer cells were incubated with redaporfin or P11 atropisomers for 24 h followed by cell lysis. Quantification of redaporfin atropisomers was inferred by redaporfin fluorescence on the supernatant of (**A**) U-2 OS, (**B**) 4T1 and (**C**) CT26 cells. Similarly, P11 atropisomers were also quantified on the supernatant of (**D**) U-2 OS, (**E**) 4T1 and (**F**) CT26 cells. Bars indicate the mean ± SEM of 2 - 3 independent experiments. Statistical significance was evaluated using one-way ANOVA *versus* the α_4 atropisomer, * $p < 0.05$ ** $p < 0.01$ and *** $p < 0.001$.

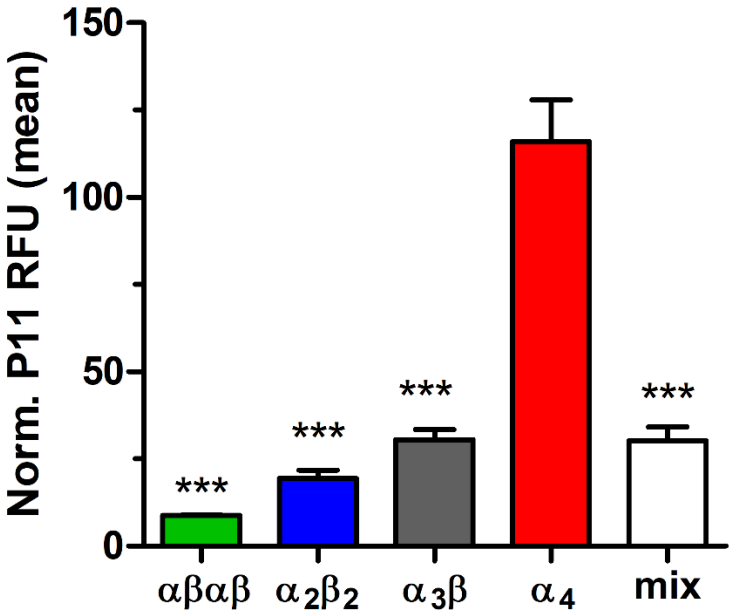

Figure S12. Cellular internalization of P11 atropisomers and P11 drug mixture. 4T1 cells were incubated with the indicated atropisomers for 24 h and cellular internalization was evaluated by flow cytometry. Bars indicate the mean ± SEM of 3 independent experiments. Fluorescence signal from treated cells was normalized to the untreated cells. Statistical significance was evaluated using two-way ANOVA *versus* the α_4 atropisomer, * $p < 0.05$ ** $p < 0.01$ and *** $p < 0.001$.

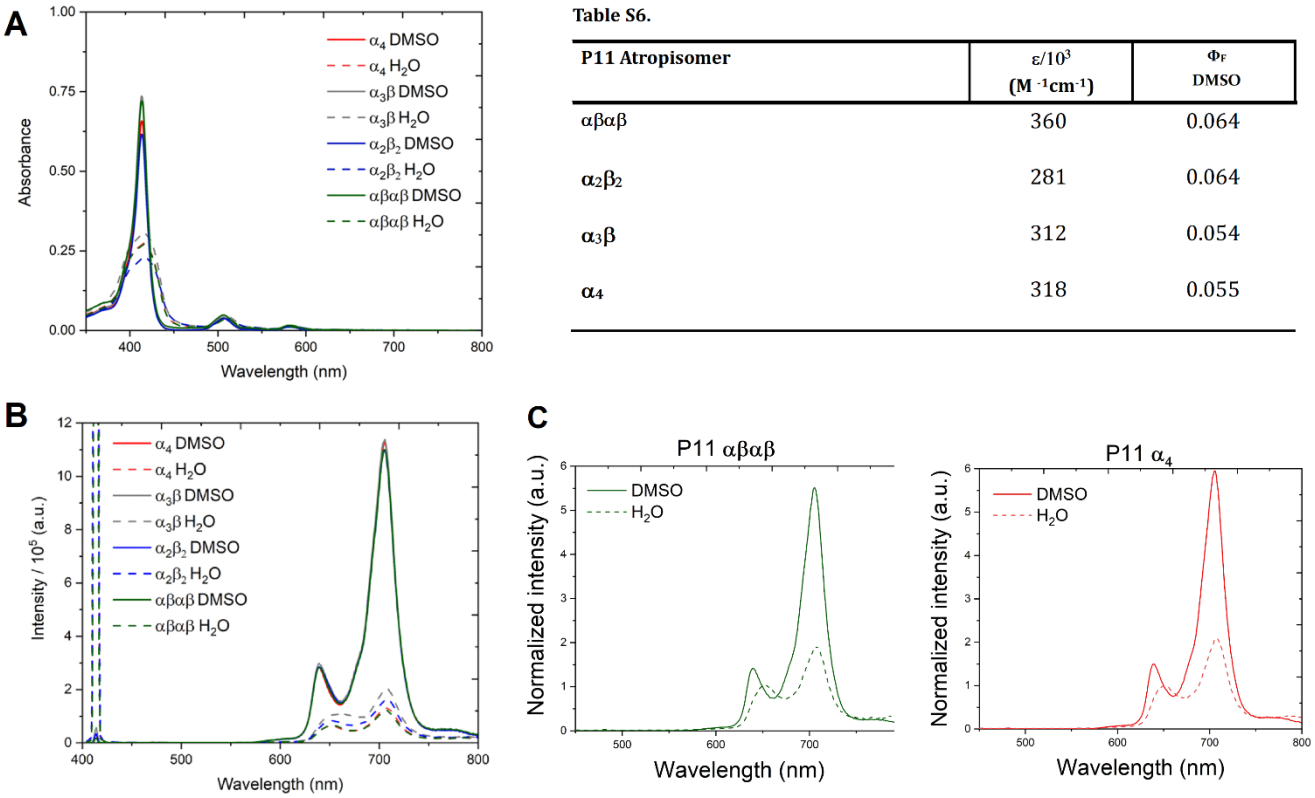

Table S6.

P11 Atropisomer	$\varepsilon/10^3$ ($M^{-1}cm^{-1}$)	Φ_F DMSO
αβαβ	360	0.064
$\alpha_2\beta_2$	281	0.064
$\alpha_3\beta$	312	0.054
α_4	318	0.055

Figure S13. P11 atropisomers aggregated similarly in aqueous solution. Steady state characterization or P11 atropisomers in H_2O (with < 1% DMSO). **(A)** Absorption spectra and **(B)** emission spectra of P11 atropisomers. **(C)** αβαβ and α_4 atropisomers emission spectra normalized to peak maxima at 605 nm. Table S6. indicates the molar absorption coefficients (ε_{max}) at 414 nm and fluorescence quantum yield Φ_F in DMSO.

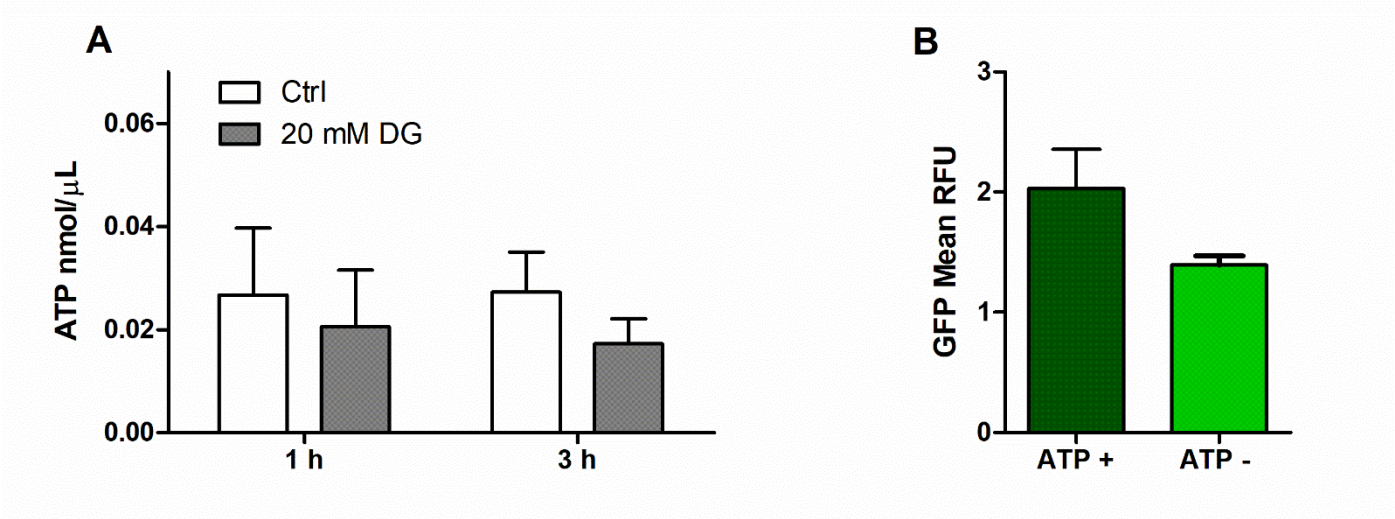

Figure S14. ATP depletion on 4T1 cells using 2-deoxy-D-glucose (DG). (A) Quantification of ATP in untreated (Ctrl) cells and following treatment with 20 mM of DG for 1 h. **(B)** Reduced GFP uptake under conditions of ATP depletion. Bars indicate the mean ± SEM of at least 3 independent experiments.

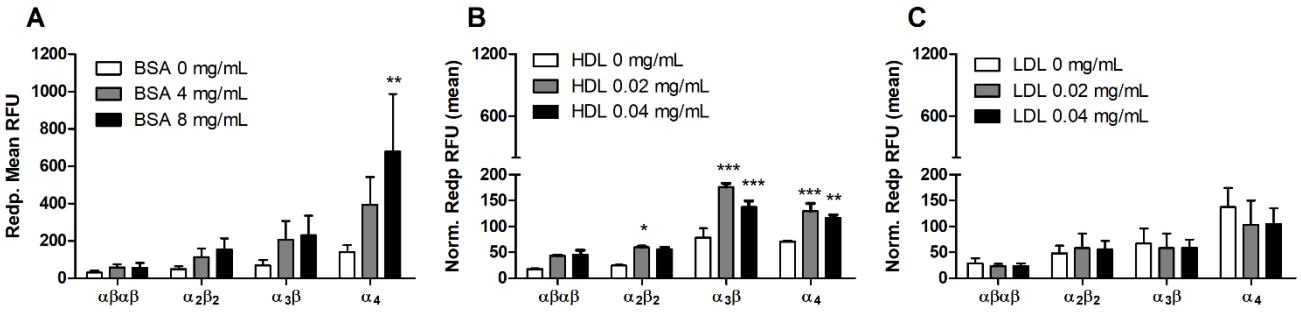

Figure S15. Internalization of redaporfin atropisomers evaluated following co-incubation for 4 h with serum proteins. (A) BSA, (B) HDL or (C) LDL; bars indicate the mean ± SEM of 3 independent experiments. Statistical significance was evaluated using two-way ANOVA * $p < 0.05$ ** $p < 0.01$ and *** $p < 0.001$.

Table S7. Dynamic light scattering results for the Kolliphor®EL formulations employed for redaporfin and P11 atropisomers. Table indicates the relative average size (z-average) of the redaporfin (saline : EtOH : Kolliphor®EL, 98.5 :1 : 0.5% v/v) and P11 (saline : DMSO : Kolliphor®EL, 97 : 1: 2% v/v) micelle size in formulations.

Redaporfin and P11 intravenous formulation

Atropisomer	Redp. Z average (nm)	P11 Z average (nm)
αβαβ	13.2 ± 0.2	14.3 ± 0.1
$\alpha_2\beta_2$	19.9 ± 6.3	13.2 ± 0.2
$\alpha_3\beta$	19.0 ± 7.9	23.8 ± 1.8
α_4	23.03 ± 3.2	18.1 ± 5.9

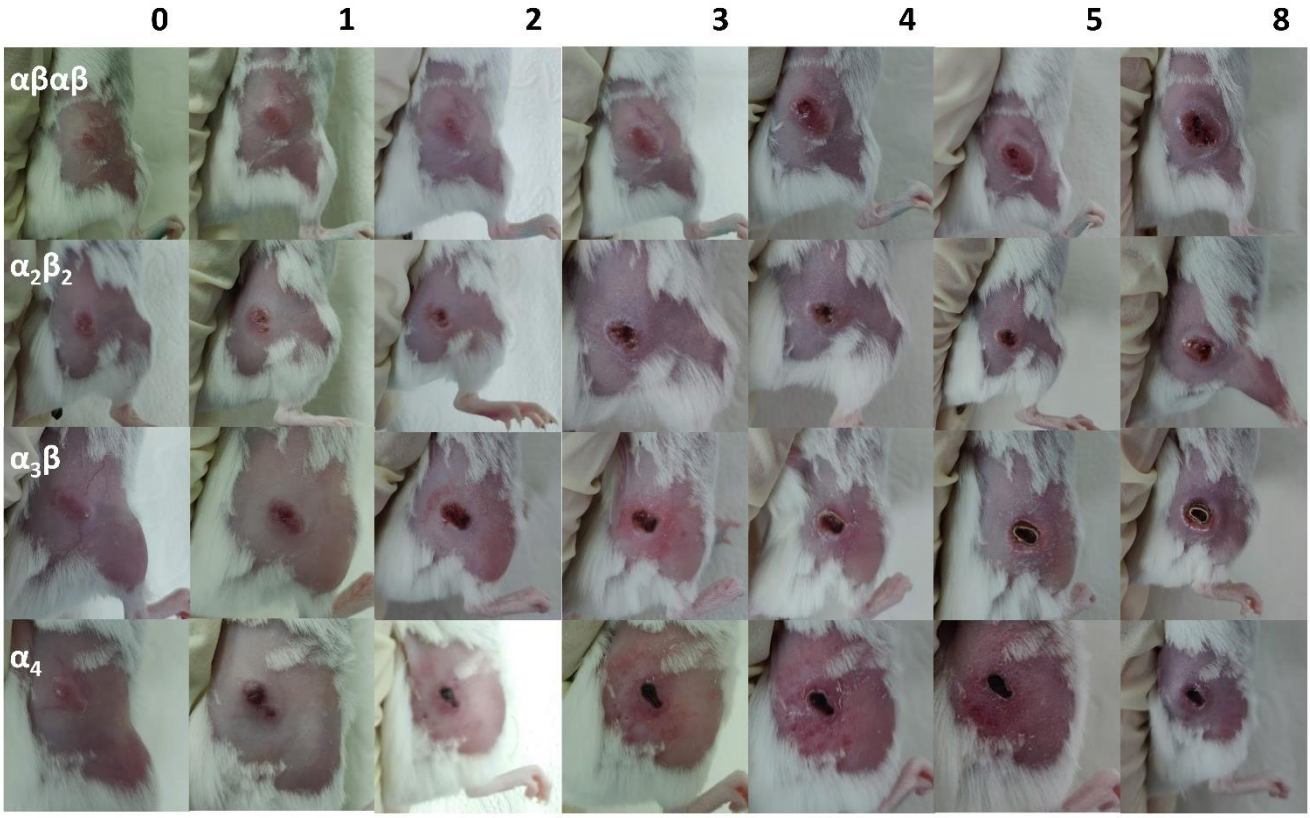

Figure S16. Representative images of CT26 tumors on female BALB/c mice 0-8 days after cellular-PDT with redaporfin atropisomers.

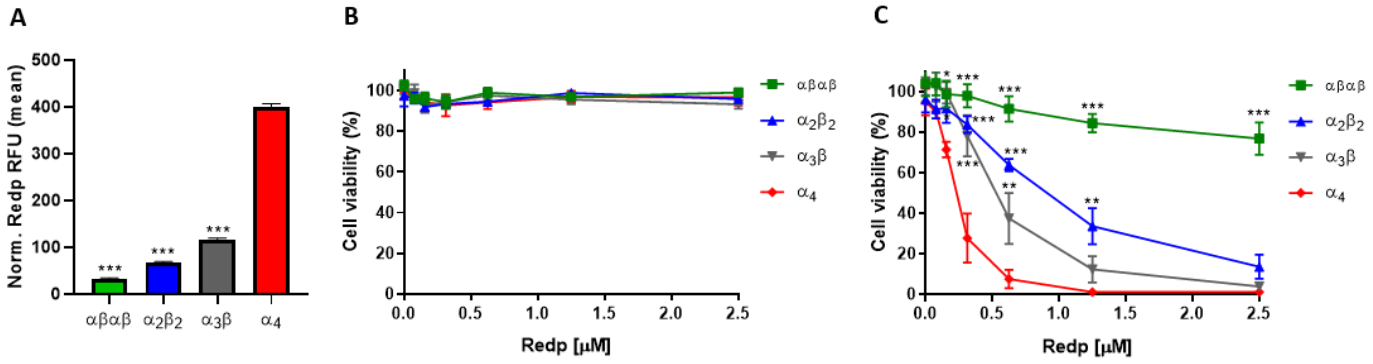

Figure S17. Cell uptake, dark toxicity and phototoxicity of redaporfin atropisomers in keratinocytes. (A) Cellular internalization of redaporfin atropisomers evaluated, by flow cytometry, after 24 h of incubation with HaCat cells. (B) Cellular viability of HaCat cells after 24 h of incubation with redaporfin atropisomers. (C) Phototoxicity of redaporfin atropisomers upon incubation with HaCat cells for 24 h and illumination with 0.2 J/cm^2. Results are expressed as the mean ± SEM of 2 independent experiments. Statistical significance was evaluated using two-way ANOVA *versus* the α_4 atropisomer, * $p < 0.05$, ** $p < 0.01$ and *** $p < 0.001$.

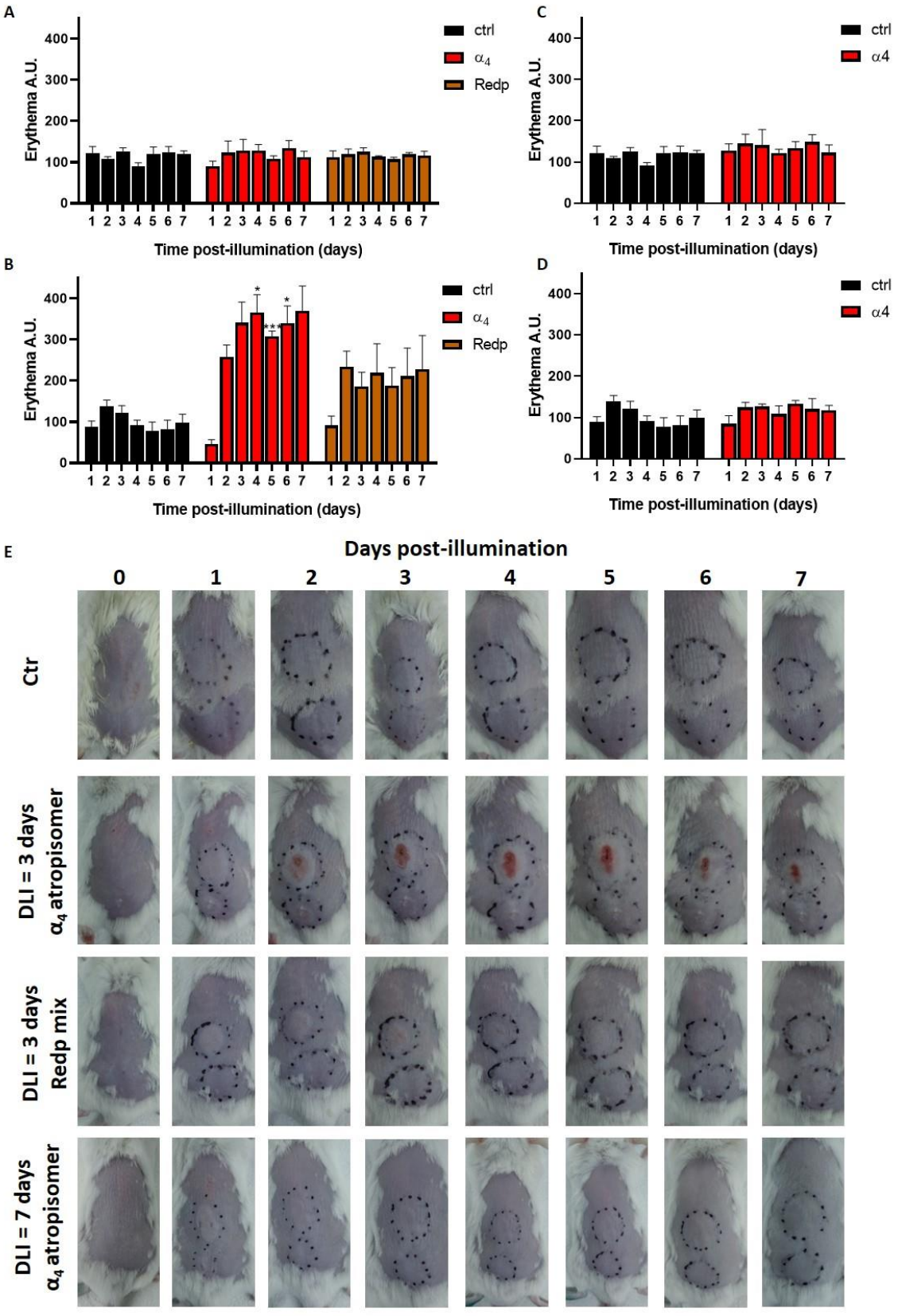

Figure S18. Skin photosensitivity of BALB/c mice after exposition to light from a solar simulator. Skin areas of 0.5 cm^2 were illuminated during 15 min (A, C) or 30 min (B, D) using a solar simulator (100 mW/cm^2) three (A,B) or seven (C,D) days post-iv administration of 0.45 mg/ Kg of α_4 or redaporfin mixture. Erythema was scored using a mexameter. Bars indicate the mean ± SEM of 3 - 4 mice, the statistical significance was evaluated using two-way ANOVA. * $p < 0.05$ and *** $p < 0.001$ *versus* ctr. **(**E) Representative images of skin effects on male Balb/c mice after exposition to light from a solar simulator.

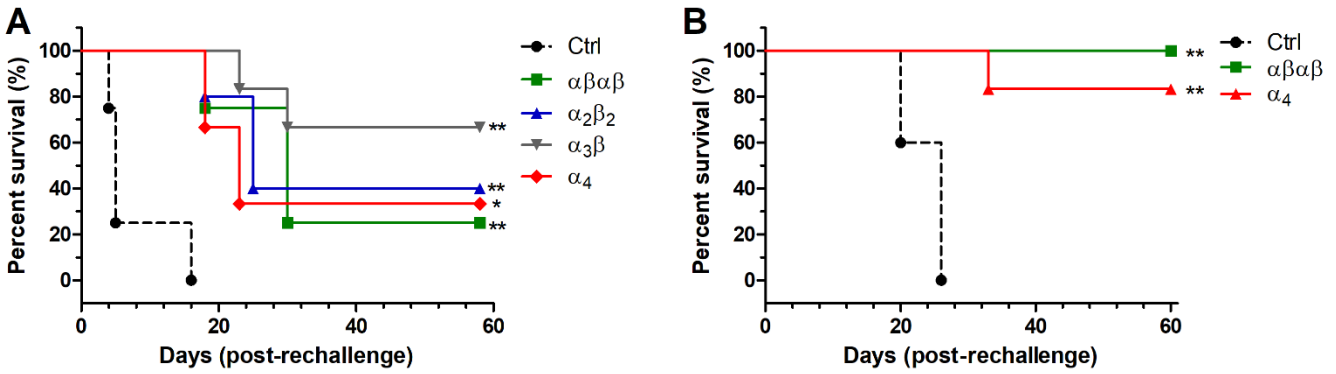

Figure S19. Immunological memory is identical for redaporfin atropisomers in vascular-PDT
Tumor protection was observed following tumor re-challenge of **(A)** female BALB/c mice (at least n = 3) and **(B)** male BALB/c mice (at least n = 5) that remained tumor-free for 60 days after vascular-PDT. Significance level was evaluated by Log-rank (Mantel-Cox) test, *versus* Ctrl mice * $p < 0.05$ and ** $p < 0.01$.

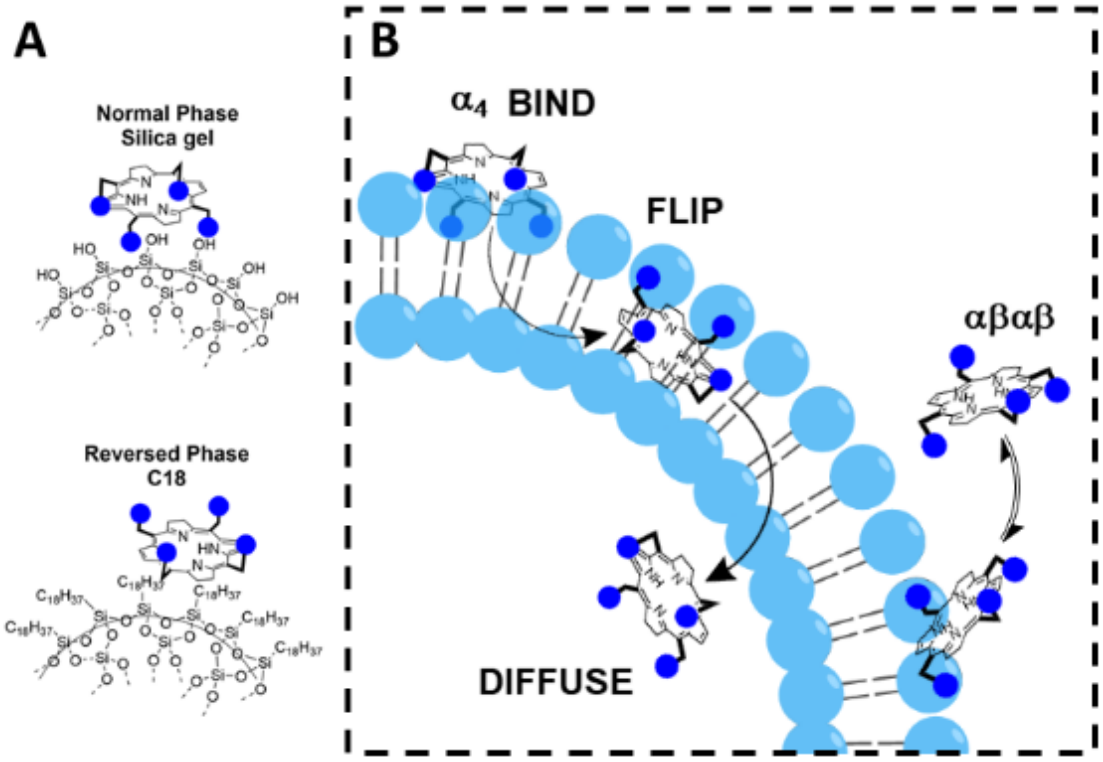

Figure S20. Schematic representation of α4 amphipathic character.
(A) Enhanced α_4 retention on normal phase silica gel and in reversed phased C18 columns. **(B)** α_4 binds to the phospholipids on the surface of the membrane, flips into the membrane to adopt the orientation of a surfactant and eventually diffuses to the interior of the cell (bind-flip mechanism). The αβαβ atropisomer is also illustrated as an equilibrium between its relatively less stable insertion in the membrane and the extracellular environment.

References

1. Goncalves, N. P. F.; Santos, T. P. C. M.; Costa, G. P. N.; Monteiro, C. J. P.; Shaberle, F.; Alfar, S. C.; Abreu, A. C. R.; Pereira, M. M.; Arnaut, L. G. Atropisomers of Halogenated Tetraphenylbacteriochlorins and Chlorins and their use in Photodynamic Therapy. WO2016151458A1, September 29, 2016.
2. *Bruker APEX-3*, v2016.9-0, Bruker AXS Inc: Madison, 2016.
3. *Bruker XREP*, Version 2014/2, Bruker AXS Inc.: Madison, 2014.
4. Hübschle, C. B.; Sheldrick, G. M.; Dittrich, B. ShelXle: A Qt Graphical User Interface for SHELXL. *J. Appl. Crystallogr*. **2011**, *44*, 1281–1284.
5. Sheldrick, G. SHELXT - Integrated space-group and crystal-structure determination. *Acta Crystallogr., Sect. A: Found. Crystallogr*. **2015,** *71*, 3-8.
6. Sheldrick, G. Crystal structure refinement with SHELXL. *Acta Crystallogr., Sect. C: Struct. Chem.* **2015**, *71*, 3-8.
7. CrystalMaker® Software, Oxford *www.crystalmaker.com*.
8. Kingsbury, C. J.; Senge, M. O. The shape of porphyrins. *Coord. Chem. Rev.* 2021, *431*, 213760.
9. Spek, A. PLATON SQUEEZE: a tool for the calculation of the disordered solvent contribution to the calculated structure factors. *Acta Crystallogr., Sect. C: Struct. Chem.* **2015,** *71*, 9-18.
10. Arnaut, L. Transitions between electronic states. In Chemical Kinetics, 2nd Ed.; Arnaut, L., Ed.; Elsevier, 2021; pp. 463-521.
11. Rurack, K.; Spieles, M. Fluorescence Quantum Yields of a Series of Red and Near-Infrared Dyes Emitting at 600−1000 nm. *Anal. Chem.* **2011,** *83*, 1232-1242.
12. Arnaut, L. G.; Pereira, M. M.; Dąbrowski, J. M.; Silva, E. F. F.; Schaberle, F. A.; Abreu, A. R.; Rocha, L. B.; Barsan, M. M.; Urbańska, K.; Stochel, G.; Brett, C. M. A. Photodynamic Therapy Efficacy Enhanced by Dynamics: The Role of Charge Transfer and Photostability in the Selection of Photosensitizers. *Chem. Eur. J.* **2014**, *20*, 5346-5357.
13. Silva, E. F.; Serpa, C.; Dabrowski, J. M.; Monteiro, C. J.; Formosinho, S. J.; Stochel, G.; Urbanska, K.; Simões, S.; Pereira, M. M.; Arnaut, L. G. Mechanisms of singlet-oxygen and superoxide-ion generation by porphyrins and bacteriochlorins and their implications in photodynamic therapy. *Chem. Eur. J.* **2010**, *16*, 9273-9286.
14. Schmidt, R.; Tanielian, C.; Dunsbach, R.; Wolff, C. Phenalenone, a universal reference compound for the determination of quantum yields of singlet oxygen $O_2(1\Delta g)$ sensitization. *J. Photochem. Photobiol., A* **1994,** *79* , 11-17.
15. Schaberle, F. A. Assessment of the actual light dose in photodynamic therapy. *Photodiagn. Photodyn. Ther.* **2018,** *23*, 75-77.
16. Czekanska, E. M. Assessment of cell proliferation with resazurin-based fluorescent dye. In *Methods in Molecular Biology*, Vol. 740; Stoddart, M., Ed.; Humana Press, 2011; pp 27-32.
17. Mantel, N. Evaluation of survival data and two new rank order statistics arising in its consideration. *Cancer Chemother. Rep.* **1966,** *50*, 163-170.